
HRP: High-Rank Preheating for Superior LoRA Initialization

Yuzhu Chen¹ Yingjie Wang² Shi Fu^{1,2} Li Shen³

Yongcheng Jing² Xinmei Tian¹ Dacheng Tao²

¹University of Science and Technology of China

²Nanyang Technological University ³Sun Yat-sen University

Abstract

This paper studies the crucial impact of initialization in Low-Rank Adaptation (LoRA). Through theoretical analysis, we demonstrate that the fine-tuned result of LoRA is highly sensitive to initialization, which is likely to lead suboptimal low-rank results. While this issue can be mitigated by adjusting the initial direction towards the main singular vectors of the target ΔW , which is, however, typically unknown in real-world scenarios. To approximate this initial direction, we propose High-Rank Preheating (HRP), which first trains LoRA with a higher preheating rank for a few steps, then uses the main singular vectors of the derived BA^\top as initialization for the main fine-tuning process. With only a modification in the initial direction, we prove that HRP makes LoRA achieve better fine-tuned results than random initialization in expectation, and the enhancement grows with the pre-heating rank. We validate our theoretical findings through extensive experiments in various models and tasks, where HRP significantly enhances LoRA’s effectiveness and outperforms other initialization strategies and other LoRA variants.

1 Introduction

Recent advances in foundation models, especially large language models, have achieved remarkable success in a diverse range of applications [4, 43, 1, 11, 12]. Nevertheless, owing to their substantial scale, the conventional full-parameter fine-tuning (FPFT) approach, where all the model’s parameters are updated for specialized tasks, has become progressively more formidable and inefficient. Parameter-efficient fine-tuning methods concentrate on integrating lightweight adapters, thus substantially diminishing computational and storage demands [20, 26, 24]. This transition not only renders the fine-tuning process more tractable but also unlocks new prospects for deploying these potent models in resource-constrained settings.

A leading technique in this area is Low-Rank Adaptation (LoRA) [20], which introduces lightweight low-rank adapters to the pre-trained weight matrices. LoRA has been extensively applied and has manifested substantial achievements in tailoring large language models [20, 30] and image generation models [10, 21] for a variety of downstream applications. Although LoRA presents significant computational benefits in practical scenarios, it still proves less effective than FPFT when computational cost is not a primary consideration [3].

To enhance LoRA’s effectiveness, many variants have emerged, with initialization improvement being one line of approach. In classic LoRA, one adapter is initialized with a zero matrix and the other with a random matrix, which makes the fine-tuning process begin with a random direction. Methods like PiSSA [31] and LoRA-GA [48] use Singular Value Decomposition (SVD) of pre-trained weights and gradients for initialization, proving the significance of LoRA initialization. However, these methods rely heavily on pre-trained models and lack theoretical guarantees for better performance, calling for more research to optimize LoRA initialization.

Delving into the optimization landscape of LoRA, this paper theoretically demonstrates that initialization plays a crucial role in achieving optimal performance. Nevertheless, random initialization leads to sub-optimal fine-tuning results, and a well-formed initialization can solve this problem. To approximate this well-formed initialization, we propose High-Rank Preheating (HRP), which further use a few steps of high-rank LoRA for enhancing initialization. Our contributions can be summarized as follows:

1. We theoretically demonstrate that initialization is important for LoRA to achieve optimal fine-tuned results. We analyze the gradient flow of classic LoRA and Asymmetric LoRA, one LoRA variant that only updates the zero-initialized matrices, and prove that: 1) with random initialization, Asymmetric LoRA can not achieve results better than random low-rank approximation in expectation, 2) classic LoRA can not achieve the best low-rank approximation from some initialization and has a similar dynamic with Asymmetric LoRA in the beginning stage, and 3) with wise initialization, both Asymmetric LoRA and classic LoRA converge exponentially to the best low-rank approximation.
2. To approach the wise initialization suggested in theory, we propose High-Rank Preheating (HRP) that employs a few more steps of Asymmetric LoRA optimization before the main fine-tuning process for superior LoRA initialization. HRP sets the main singular vectors of the derived BA^\top as LoRA initial directions, which approximate the main singular vectors of the target ΔW . With only a modification in initialization, we prove that HRP makes LoRA achieve better converged results than random initialization in expectation.
3. To validate our theoretical findings and evaluate the effectiveness of HRP, we conducted experiments on natural language understanding (NLU) tasks and natural language generation (NLG) tasks across various models. In the results, HRP makes LoRA outperform most of its other variants and achieves comparable performance with full-parameter fine-tuning, demonstrating its effectiveness in real-world scenarios. With suitable hyperparameters, HRP requires relatively negligible more time and no more GPU memory.

2 Related Work

Role of initialization. Parameter initialization is one of the initial elements that largely account for the final model performance [13, 33]. Existing initialization methods are designed to control the norms of network parameters via Gaussian initialization [17] or orthonormal matrix initialization [38] with different variance patterns. Currently, learning-based initialization methods are explored: [8] proposes to optimize the curvature, [56] suggests optimizing the loss reduction of the first stochastic step, while [51] optimizes the cosine similarity of sample-wise gradients.

The initialization for LoRA is also a hot topic in previous research. [15] study the difference between the left sketch and the right sketch from a stability perspective. [5] leverages orthonormal matrix initialization through QR decomposition. [31, 48] initialize adapters with the principal components of the weight matrices and their gradients in pre-trained models. [25] brings Nyström initialization to LoRA for better convergence. Compared to these works, our method does not require further knowledge or pre-trained weights.

LoRA variations. Since introducing the original LoRA technique [20], various efforts have been made to enhance LoRA further. [55] adaptively allocates the parameter budget among weight matrices. [57] freezes the random-initialized matrices for better generalization. [50, 29] suggest using a chain of LoRA for better expressive power. To further decrease the number of trainable parameters, [2, 35] suggest injecting small matrices between LoRA blocks, and [23, 37, 39] suggest sharing LoRA weights across different modules. Compared to these works, this paper focuses on enhancing LoRA from the perspective of initialization.

Matrix factorization. We also note some works about matrix factorization here. Matrix factorization considers approximating a target matrix by two multiplied matrices [6]. Theoretical works show that this training paradigm converges in both symmetric [40, 32] and asymmetric [52, 49] settings when adapters are initialized to small random matrices and the target has low rank. Compared to these works, this paper focuses more on the realistic setting for LoRA, where the target may have a high rank and initialization is not small.

3 Theory: Why Initialization Matters

In this section, we investigate the gradient flow of LoRA, demonstrating how its initialization influences the fine-tuned result. In the setting of matrix factorization, we show that LoRA with random initialization performs poorly in subsection 3.2 while LoRA with wise initialization performs well in subsection 3.3.

3.1 Framework

LoRA [20] adapts pre-trained models by updating weights through the product of two low-rank matrices scaled by a multiplier. Specifically, for a sub-module $W^{\text{pre}} \in \mathbb{R}^{b \times a}$ in the pre-trained model, a r -rank LoRA takes $A \in \mathbb{R}^{a \times r}$ and $B \in \mathbb{R}^{b \times r}$ as adapters, and the weight adaption is given by

$$W^{\text{init}} \rightarrow W^{\text{init}} + \frac{\alpha}{r} BA^{\top},$$

where α denotes the scaling factor and the initial weights $W^{\text{init}} = W^{\text{pre}}$ are kept frozen during optimization. Only the parameters of A and B are updated through optimization algorithms.

In this paper, we study the initialization of A and B through gradient flow, which approximates gradient descent. For loss function \mathcal{L} , the update rule of gradient descent is given by:

$$A_{t+1} = A_t - \frac{\eta_A \alpha}{r} \nabla_W \mathcal{L} \left(W + \frac{\alpha}{r} B_t^{\top} A_t \right)^{\top} B_t, \quad B_{t+1} = B_t - \frac{\eta_B \alpha}{r} \nabla_W \mathcal{L} \left(W + \frac{\alpha}{r} B_t^{\top} A_t \right) A_t,$$

where η_A is the learning rate for optimizing A while η_B is for B . When the learning rate is sufficiently small, the update rule is a first-order approximation of the gradient flow:

$$\dot{A}_t = -\eta_A G_t^{\top} B_t, \quad \dot{B}_t = -\eta_B G_t A_t, \quad (1)$$

where G_t denotes gradient $\frac{\alpha}{r} \nabla_W \mathcal{L} \left(W + \frac{\alpha}{r} B_t^{\top} A_t \right)$, notion \dot{A}_t denotes $\frac{dA_t}{dt}$ and \dot{B}_t is defined similarly.

For the initialization of A_t and B_t , **zero+random initialization schema** is widely used in LoRA, where one adapter is initialized to a zero matrix and another to a random matrix. Every element in the random-initialized matrix is independently and identically distributed from a Gaussian distribution $\mathcal{N}(0, \sigma^2)$. We call the $A_0 = O_{a \times r}$ case left sketch initialization (LSI) and the $B_0 = O_{b \times r}$ case right sketch initialization (RSI). [57] suggest orthogonal initialization, which replaces the Gaussian matrix with its top r singular vectors and demonstrates similar performance to Gaussian initialization.

Updating A with η_A while updating B with η_B is suggested by [16], which contains two special and widely-used subcases: 1) **classic LoRA** where $\eta_A = \eta_B = \eta$, and 2) **Asymmetric LoRA** where $\eta_A = 0, \eta_B = \eta$ for RSI and $\eta_A = \eta, \eta_B = 0$ for LSI. The classic LoRA is the original version proposed in [20]. Asymmetric LoRA is a variant that freezes the random-initialized matrix, which reduces the number of trainable parameters and allows a higher rank. In this paper, we focus on how A_0, B_0 affect the performance of A_t, B_t under these two updating strategies.

3.2 Random initialization leads bad performance

As studied in [54], the expressive power of LoRA for fully connected neural networks and the Transformer architecture requires the capability of achieving the best low-rank approximation to some well-trained sub-modules during optimization (the analysis is optimization-free and thus also applicable for Asymmetric LoRA). Formally, for a target model W^{target} , LoRA adapter $\frac{\alpha}{r} B_t A_t^{\top}$ is expected to achieve the best rank- r approximation of $W^{\text{target}} - W^{\text{init}}$.

This expected problem is expressed well in the problem of matrix factorization, where the loss function is the Frobenius norm toward the target. With no loss of generality, we consider $W^{\text{init}} = O_{b \times a}$ while treating $M = W^{\text{target}} - W^{\text{init}}$ as target for $\frac{\alpha}{r} B_t A_t^{\top}$. Then, the loss function \mathcal{L} and gradient G_t can be expressed as

$$\mathcal{L}_t = \frac{1}{2} \left\| \frac{\alpha}{r} B_t A_t^{\top} - M \right\|_F^2, \quad \text{and} \quad G_t = \frac{\alpha}{r} \left(\frac{\alpha}{r} B_t^{\top} A_t - M \right). \quad (2)$$

According to Eckart-Young Theorem [9], the global minima to $\frac{\alpha}{r} B^\top A$ is the best rank- r approximation of M , with minimum loss as follows:

$$\left(\frac{\alpha}{r} B A^\top\right)^* = \sum_{i=1}^r \sigma_i(M) u_i(M) v_i(M)^\top, \quad \mathcal{L}^* = \frac{1}{2} \sum_{i=r+1}^{\min\{a,b\}} \sigma_i(M)^2$$

where $\sigma_i(M)$ is the i -th large singular value of M and $u_i(M), v_i(M)$ are the corresponding left and right singular vector. With no loss of generality, we assume the singular values of M are different from each other. For expressive power in more complex tasks, LoRA is expected to at least achieve some points with loss similar to \mathcal{L}^* in the setting of matrix factorization. Unfortunately, we show that fine-tuned results of Asymmetric LoRA and classic LoRA are likely to have a significantly higher loss.

Asymmetric LoRA struggles to perform well. We begin by examining the optimization landscape of Asymmetric LoRA [57]. Due to the fixed random-initialized LoRA adapter, the derived $\frac{\alpha}{r} B_t A_t$ is limited by the direction of the frozen adapter, which is always not fit to target M . Theoretically, we show that when the frozen adapter is randomly settled, the expectation loss of Asymmetric LoRA is lower bounded by the loss of random rank- r approximation, which is sometimes much higher than \mathcal{L}^* . Specifically, we have the following theorem.

Theorem 1. *Consider Asymmetric LoRA under objective 2 in gradient flow 1 with the frozen adapter from Gaussian initialization or orthogonal initialization. For LSI and RSI, we have for all $t > 0$:*

$$\mathbb{E}_{LSI} [\mathcal{L}_t] \geq \frac{b-r}{2b} \sum_{i=1}^{\min\{a,b\}} \sigma_i(M)^2, \quad \mathbb{E}_{RSI} [\mathcal{L}_t] \geq \frac{a-r}{2a} \sum_{i=1}^{\min\{a,b\}} \sigma_i(M)^2,$$

where \mathbb{E} represents the expectation with respect to randomness in initialization. The inequality becomes an equality when $t \rightarrow \infty$.

Proof is included in Appendix A.2. Theorem 1 shows that from the perspective of expectation loss, Asymmetric LoRA can not achieve results better than random rank- r approximation with a random frozen adapter. Compared with the best rank- r approximation, the lower bound is much higher than \mathcal{L}^* when the singular values of target M diverge a lot, e.g. when M has low effective rank. As observed by [47], the rank-dimension ratio of well-trained neural networks is usually relatively small, indicating a low effective rank structure for both W^{pre} and W^{target} , thus also for $M = W^{\text{target}} - W^{\text{init}}$. Therefore, under zero+random initialization schema, the performance of Asymmetric LoRA is always much less than is expected.

Besides, we acknowledge that the lower bound of Theorem 1 decreases linearly with the LoRA rank r . This decreasing rate is more pronounced than that of \mathcal{L} , suggesting that the performance gap to the best rank- r approximation diminishes as r increases. Therefore, employing a higher rank in Asymmetric LoRA is a way to enhance performance. Specifically, when using Asymmetric LoRA with full rank ($r = \min a, b$), it can converge to global minima with probability one. However, totally using higher rank for main fine-tuning process is equivalent to FPFT, which needs more computation and GPU memory usage in practical applications.

Compared with other theoretical works in matrix factorization [40, 32, 52, 49], which demonstrates that the gradient flow of matrix factorization converges to global minima, our approach suggests a different conclusion because of difference in the following ways: 1) we allow the target matrix M to be of high rank, which may not be fully approximate-able by a low-rank matrix $\frac{\alpha}{r} B A^\top$; 2) we consider the case where adapter matrices are initialized as zero and random, respectively, whereas the aforementioned works assume both matrices are initialized with small random values; and 3) our objective is Asymmetric LoRA, where only one matrix is optimized, which is different from their approaches.

Classic LoRA has similar properties. Different from Asymmetric LoRA, classic LoRA lets the random-initialized to be updated, thus has more trainable parameters and is more expressive. Though theory papers in matrix factorization [40, 32, 52, 49] suggest that optimizing both A and B results in converging to M with high probability when both A and B are initialized from small random matrices, we demonstrate that under zero+random initialization and fine-tuning schema, classic LoRA also struggles to perform well. First, we show that for some special initialization, classic LoRA can not achieve to the best low-rank result in matrix factorization.

Theorem 2. For classic LoRA under objective 2 in gradient flow 1, if there exists $i \leq r$ making the initial A_0 and B_0 satisfy $A_0^\top v_i(M) = O_a$ and $B_0^\top u_i(M) = O_b$, we have for all $t \geq 0$:

$$\left(\frac{\alpha}{r} B_t A_t^\top\right) v_i = O_b, \quad \text{and} \quad u_i^\top \left(\frac{\alpha}{r} B_t A_t^\top\right) = O_a^\top,$$

resulting in for all $t \geq 0$:

$$\mathcal{L}_t - \mathcal{L}^* \geq \frac{1}{2} [\sigma_i(M)^2 - \sigma_{r+1}(M)^2] > 0,$$

where $\sigma_i(M)$ is the i -th large singular value of M and $u_i(M), v_i(M)$ are the corresponding left and right singular vector.

Proof is included in Appendix A.3. Theorem 2 shows that when the initialization of LoRA lies on a subspace orthogonal to some $u_i(M)v_i(M)^\top$ from the target, the orthogonal property will always hold in X_t , leading to a failure in converging to the best low-rank result. In zero+random initialization, the orthogonal property to the zero-initialized adapter is always satisfied ($A_0^\top v_i(M) = O_a$ for LSI and $B_0^\top u_i(M) = O_b$ for RSI). This means that once the random-initialized matrix is orthogonal to some main singular vectors of the target, classic LoRA can never achieve the best rank- r approximation. The target is always unknown in the initializing stage, thus these bad directions can not be easily avoided from random initialization.

Aside from these specific initialization directions, we also observe that classic LoRA has a similar optimization dynamic with Asymmetric LoRA when the fine-tuning process is not sufficiently comprehensive, thus sharing similar properties including sub-optimal performance. This similar dynamic is empirically supported by experiments [57] where Asymmetric LoRA obtains similar results with classic LoRA in real-world scenarios. To theoretically demonstrate this similarity, we have the following theorem.

Theorem 3. Consider the gradient flow of classic LoRA B_t, A_t and that of Asymmetric LoRA \tilde{B}_t, \tilde{A}_t in the same zero+random initialization. Assume computed gradient G_t is bounded by R and is Lipschitz in the Frobenius norm, then the difference between Asymmetric LoRA and classic LoRA is upper bounded by

$$\left\| \frac{\alpha}{r} B_t A_t^\top - \frac{\alpha}{r} \tilde{B}_t \tilde{A}_t^\top \right\|_F = O(\eta^4 R^3 r t^4), \quad (3)$$

for small t when they are under a same gradient calculator.

Proof is included in Appendix A.4. In fine-tuning tasks, pre-trained models have already acquired powerful capabilities from training on other tasks, enabling their effectiveness in real-world applications. Therefore, the fine-tuning stage is expected to make only modest modifications to the model parameters, making the assumption of bounded gradient norm reasonable. Additionally, assuming the gradient calculator is Lipschitz in the Frobenius norm is justified because the backward propagation process of neural networks exhibits this property in bounded domains. Besides, this Lipschitz assumption is widely adopted in other theoretical works [34].

Theorem 3 tells that in many fine-tuning tasks, classic LoRA exhibits dynamics similar to Asymmetric LoRA with the same zero+random initialization, particularly during the early stages of training (small t). As addressed above, Asymmetric LoRA tends to achieve random low-rank results rather than the best low-rank approximation. Given this dynamic similarity, classic LoRA inherits the same limitation when the fine-tuning process is not sufficiently comprehensive.

3.3 Wise initialization leads good convergence

Then, we illustrate that the above limitation of Asymmetric LoRA and classic LoRA is mainly attributed to initialization. Specifically, we show that by merely altering the random initialization to a well-formed direction, both Asymmetric LoRA and classic LoRA converge to the global minima exponentially in the matrix factorization problem.

Theorem 4. Consider Asymmetric LoRA under objective 2 in gradient flow 1. For RSI with $A_0 = \sum_{i=1}^r v_i(M) e_{i,r}$, $B_0 = O_{b \times r}$ or LSI with $A_0 = O_{a \times r}$, $B_0 = u_i(M) e_{i,r}$, we have

$$\mathcal{L}_t - \mathcal{L}^* = O(\exp\{-2\alpha\eta t/r\}),$$

where $v_i(M)$ and $u_i(M)$ are the i -th right and left singular vector of M and are defined in Theorem 2. $e_{i,r}$ is the $1 \times r$ vector with the i -th element being 1 and all other elements being 0.

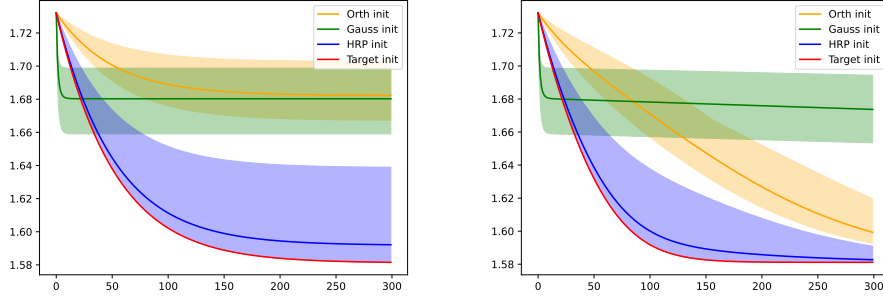


Figure 1: Loss curves for matrix factorization targeting $M = \text{diag}(I_{12}, O_{20 \times 20})$ with $r = 2$. Left: classic LoRA in Gaussian initialization, orthogonal initialization, HRP derived initialization with $hrp_rank = 6$, and target initialization (suggested in Theorem 4). Right: Asymmetric LoRA in the same initialization strategies.

Proof is included in Appendix A.5. Theorem 4 shows that when initialized with the main singular vectors of the target, Asymmetric LoRA has exponential convergence to the best rank- r approximation of M . Compared with Theorem 1, the only difference in the setting lies in the initialization. Meanwhile, the conclusion shifts from ‘can not perform better than random rank- r approximation’ to ‘converges to the best rank- r approximation exponentially’. Therefore, the performance limitation of Asymmetric LoRA is attributed to random initialization. Furthermore, when the initialization is appropriately configured, optimizing a single LoRA adapter while freezing another one is sufficient to ensure performance in matrix factorization.

Theorem 5. *Consider classic LoRA under objective 2 in gradient flow 1. For initialization same as Theorem 4, we have*

$$\mathcal{L}_t - \mathcal{L}^* = O \left(\exp \left[-\frac{2\alpha\eta t}{r} - \frac{\alpha\eta t}{r} \left(-1 + \sqrt{1 + \frac{2r^2}{\alpha^2} \sigma_r(M)^2 \left[1 - e^{-\frac{\alpha\eta t}{2r}} \right]^2} \right) \right] \right),$$

where $\sigma_i(M)$ is the i -th singular value of M and is defined in Theorem 2.

Proof is included in Appendix A.6. Theorem 5 demonstrates that the initialization suggested in 4 also makes classic LoRA converge to the best rank- r result exponentially, thereby avoiding the unfavorable scenario described in Theorem 2. Similar to analysis in Asymmetric LoRA, the performance limitation of classic LoRA is also attributed to random initialization. It is also noteworthy that with the same well-formed initialization, the convergence rate of classic LoRA has an extra positive term $\frac{\alpha\eta t}{r} \left(-1 + \sqrt{1 + \frac{2r^2}{\alpha^2} \sigma_r(M)^2 \left[1 - e^{-\frac{\alpha\eta t}{2r}} \right]^2} \right)$ from the convergence rate of Asymmetric LoRA, indicating a better fine-tuned result in the perspective of convergence.

In practice with pre-trained model modules W^{pre} and its well fine-tuned version W^{target} , LoRA is expected to make each $\frac{\alpha}{r} B_i A_i^\top$ a best rank- r approximation of $W_i^{\text{target}} - W_i^{\text{pre}}$. However, calculating the SVD decomposition of $W_i^{\text{target}} - W_i^{\text{pre}}$ is always impossible because W_i^{target} is unknown. Previous work proposes some initialization methods for LoRA, such as PiSSA [31] and LoRA-GA [48]. PiSSA [31] considers using main singular vectors of W^{pre} as initialization while LoRA-GA [48] suggests using main singular vectors of $\nabla_{W^{\text{pre}}} \mathcal{L}(W^{\text{pre}})$. Their methods rely on the information from a single weight point W^{pre} , which could be easily affected by noise from the pre-trained model and gradient noise.

4 Method: High-Rank Preheating

Though Asymmetric LoRA can not achieve the best rank- r approximation of the target directly, it does approximate the target in some random direction, thus bringing out some information about the target implicitly. HRP leverages this implicit information to approximate the wise initialization

suggested in Theorem 4. Specifically, when using the RSI strategy, HRP can be formulated as Algorithm 4.

Algorithm 1 High-Rank Preheating for RSI

Input: HRP parameters hrp_rank , hrp_step and hrp_bs , rank r for LoRA, pre-trained model W

1: Select random orthogonal matrix $\hat{U} \in \mathbb{R}^{b \times b}$ with i -th column \hat{u}_i

2: High-rank preheating in batch size hrp_bs :

$$\hat{A}, \hat{B}_0 \leftarrow \text{hrp_step steps AsymLoRA with LSI: } \hat{A}_0 = O_{a \times r}, \hat{B}_0 = \sum_{i=1}^{\text{hrp_rank}} \hat{u}_i e_{i, \text{hrp_rank}}^\top$$

3: Calculate first r right singular vectors $v_i(\hat{B}_0 \hat{A}_0^\top)$ for $i = 1, \dots, r$

4: Fine-tuning

$$A, B \leftarrow \text{LoRA fine-tuning with RSI: } A_0 = \sum_{i=1}^r v_i(\hat{B}_0 \hat{A}_0^\top) e_{i,r}^\top, \hat{B}_0 = O_{b \times r}$$

Output: fine-tuned model $W + \frac{\alpha}{r} B A^\top$

To illustrate why HRP approximates the well-formed initialization, we take LoRA for RSI in matrix factorization as an example, where the well-formed initialization requires the main r right singular vectors to initialize A . One step HRP updates \hat{A}_0 from $O_{a \times r}$ to

$$\hat{A}_1 = \hat{A}_0 - \frac{\eta_A \alpha}{r} \nabla_W \mathcal{L} \left(W + \frac{\alpha}{r} \hat{B}_0^\top \hat{A}_0 \right)^\top \hat{B}_0 = \frac{\eta \alpha}{r} M^\top \hat{B}_0,$$

while the derived ΔW updates from $\frac{\alpha}{r} \hat{B}_0 \hat{A}_0^\top = O_{b \times a}$ to

$$\frac{\alpha}{r} \hat{B}_1 \hat{A}_1^\top = \frac{\eta \alpha^2}{r^2} \hat{B}_0 \hat{B}_0^\top M = \frac{\eta \alpha^2}{r^2} \hat{U} \begin{pmatrix} I_{\text{hrp_rank}} & \\ & O_{(b-\text{hrp_rank}) \times (b-\text{hrp_rank})} \end{pmatrix} \hat{U}^\top M.$$

Due to the random selection of \hat{U} , $\frac{\alpha}{r} \hat{B}_1 \hat{A}_1^\top$ tends to have similar main singular vectors with M . With a higher hrp_rank , more effective directions from \hat{U} are used for approaching M , thus approaching M better. Specifically, we prove that HRP achieves the initialization that leads to better converged results in matrix factorization.

Theorem 6. *For any $\text{hrp_step} > r$ in objective 2 with gradient flow, HRP initialization makes Asymmetric LoRA converge to results with expectation loss*

$$\mathbb{E}_{\text{HRP}} \mathcal{L}_\infty \leq \sum_{i=r+1}^{\text{hrp_rank}} \sigma_i(M)^2 + \frac{a - \text{hrp_rank}}{2a} \sum_{i=1}^{\max(a,b)} \sigma_i(M)^2.$$

Proof is included in Appendix A.7. Compared with the lower bound of Theorem 1, the upper bound of expectation loss in Theorem 6 modifies $\text{hrp_rank} - r$ terms of the averaged singular value with $r + 1$ -th to hrp_rank -th singular value. This means that when the target $W^{\text{target}} - W^{\text{pre}}$ has a small effective rank, which is observed by [46, 47] in practice, HRP improves the converged result a lot. Besides, we note that the upper bound is decreasing with hrp_rank growing, which is why we use a higher rank for preheating.

Aside from theoretical analysis, we conduct numerical experiments and show results in Figure 1. As shown, HRP indeed achieves better performance than random initialization, while approaching the performance of target initialization.

In real-world scenarios, HRP requires some modifications for fit more complex problems. Firstly, to mitigate the problem of gradient noise, HRP needs more than one preheating step in real-world experiments. Besides, HRP uses high rank Asymmetric LoRA, which requires more GPU memory. To mitigate this problem, we select a smaller batch size in the HRP process to save GPU memory cost. Furthermore, calculating SVD decomposition is sometimes of high cost when dealing with wide neural networks. To accelerate HRP, we use the random SVD algorithm [44] in step 3 of Algorithm 4.

Table 1: Results with T5-base on tasks from a subset of the GLUE benchmark. **Blue** marked denotes the best result across different initialization, while **red** marked denotes the best result over all baselines.

	CoLA	MRPC	QNLI	RTE	STS-B	Avg.
AdaLoRA	54.78 \pm 1.83	88.64 \pm 0.31	92.68 \pm 0.07	74.13 \pm 1.62	88.50 \pm 0.31	79.75 \pm 0.40
rsLoRA	54.91 \pm 1.06	89.05 \pm 0.31	92.07 \pm 0.13	73.29 \pm 0.88	89.17 \pm 0.16	79.70 \pm 0.26
DoRA	54.61 \pm 1.87	88.40 \pm 1.10	91.96 \pm 0.07	73.85 \pm 0.17	88.93 \pm 0.36	79.55 \pm 0.53
FPFT	55.85 \pm 0.64	89.46 \pm 1.06	92.50 \pm 0.14	74.01 \pm 1.93	89.34 \pm 0.57	80.23 \pm 0.42
LoRA	54.93 \pm 1.59	88.32 \pm 0.81	91.96 \pm 0.19	73.65 \pm 2.06	88.83 \pm 0.39	79.54 \pm 0.78
LoRA (orth)	54.84 \pm 0.27	88.48 \pm 0.53	91.95 \pm 0.16	73.89 \pm 2.74	88.87 \pm 0.11	79.60 \pm 0.57
PiSSA	55.30 \pm 0.53	88.73 \pm 1.00	91.74 \pm 0.27	73.04 \pm 1.62	88.54 \pm 0.21	79.47 \pm 0.64
LoRA-GA	53.04 \pm 1.22	88.64 \pm 0.81	92.13 \pm 0.13	72.08 \pm 2.01	88.84 \pm 0.39	78.95 \pm 0.53
HRP (ours)	56.18 \pm 0.09	88.89 \pm 0.61	92.23 \pm 0.08	74.25 \pm 1.90	89.04 \pm 0.16	80.12 \pm 0.52

Compared with totally fine-tuning with high-rank LoRA, HRP maintains the same number of trainable parameters as low-rank LoRA in the main fine-tuning process, thereby preserving the better generalization guarantee against totally high-rank LoRA (refer to Lemma 4.5 in [57] where generalization error is upper bounded by $O(\sqrt{r})$). Furthermore, with the decreased batch size in HRP, it costs much more time for totally fine-tuning high-rank LoRA with the same epochs as HRP-initialized low-rank LoRA.

We also compare HRP with other LoRA initialization - PiSSA [31] and LoRA-GA [48], where neither A_0 nor B_0 is initialized as a zero matrix and W^{init} is settled to $W^{\text{pre}} - \frac{\alpha}{r} B_0 A_0^\top$ to ensure that $W + \Delta W$ is fine-tuned from W^{pre} . This has implications for checkpoint storage, where sometimes only the trained LoRA weights need to be shared. While with these methods, either both B^{init} , A^{init} and B^{tuned} , A^{tuned} need to be stored, or the weights must be merged, both of which require more memory. Compared with their methods, HRP keeps the properties $B_0 A_0^\top = O_{b \times a}$ and $W^{\text{init}} = W^{\text{pre}}$ from LoRA, thus does not require more checkpoint storage.

5 Experiments

In this section, we validate the effectiveness of HRP through experiments. We compare HRP with several baselines to demonstrate its effectiveness: 1) Full-Parameter Fine-Tuning (FPFT): updates all model parameters from pre-trained weights; 2) other LoRA variants, including: 2.1) DoRA [27]: with additional learnable magnitudes, 2.2) rsLoRA [22]: with a scaling factor for stability, and 2.3) AdaLoRA [55]: with dynamically adjusted rank allocation; and 3) classic LoRA with different initialization methods: 3.1) kaiming normal initialization, 3.2) orthogonal initialization [57], 3.3) PiSSA [31]: first r main singular vectors of W^{pre} , and 3.4) LoRA-GA [48]: first $2r$ main singular vectors of gradient approximation.

5.1 Experiments on NLU tasks

We first evaluate the performance of HRP and other LoRA variants under the natural language understanding (NLU) tasks. Specifically, we fine-tune the T5-base model [36] on a subset of GLUE [45] benchmark, including CoLA, MRPC, QNLI, RTE, and STS-B. For all variants of LoRA, we inject LoRA blocks to all query and value sub-modules with low rank $r = 4$ and $\alpha = r$. For HRP, we set `hrp_rank` = 128, `hrp_bs` = 16, and `hrp_step` = 100 with the same training dataset as the main fine-tuning process. We present more implementation details in Appendix B.

Results are shown in Table 1 where performance is evaluated on the Matthews correlation coefficient for CoLA, Pearson correlation coefficient for STS-B, and accuracy for the remaining tasks. Each experiment is conducted for 3 different random seeds (fixed seeds across different methods), and both the average and standard deviation are reported. As demonstrated, HRP outperforms all other initialization strategies and most of the other variants while achieving results comparable to FPFT. Besides, we report the time and GPU cost in Table 3. As shown, HRP costs negligible time compared to the subsequent fine-tuning process, while it needs no more GPU memory. To study how HRP hyperparameters affect the fine-tuned result, we include ablation studies in Appendix C.1.

Table 2: Results with LLMs on math reasoning tasks. **Blue** marked denotes the best result across different initialization, while **red** marked denotes the best result over all baselines.

	GSM8K				MATH			
	Llama	Qwen	Gemma	Avg.	Llama	Qwen	Gemma	Avg.
AdaLoRA	44.73	69.98	54.44	56.38	15.70	25.72	15.68	19.03
rsLoRA	45.72	69.14	53.75	56.20	14.90	26.62	14.86	18.79
DoRA	48.37	70.13	56.18	58.23	15.08	26.84	16.26	19.39
FPFT	46.93	71.49	49.66	56.03	12.78	26.84	10.76	16.79
LoRA	44.88	69.22	51.93	55.34	13.64	23.48	13.42	16.85
LoRA (orth)	41.77	66.11	41.39	49.76	11.12	22.16	10.30	14.53
PiSSA	47.08	70.89	56.10	58.02	15.10	26.52	16.42	19.35
LoRA-GA	48.29	69.98	56.48	58.25	14.54	26.88	15.54	18.99
HRP (ours)	48.67	70.66	58.38	59.24	15.62	27.24	15.98	19.61

Table 3: Time and GPU memory cost of LoRA-GA, HRP, and the following fine-tuning process. We report the computational cost with QNLI for T5-base while MetaMathQA for other models.

	Time (s)				GPU Memory (MB)			
	T5-base	Llama	Qwen	Gemma	T5-base	Llama	Qwen	Gemma
HRP	15	88	95	117	5106	24414	35080	53560
Main tuning	3194	1721	2769	3626	8040	38702	56368	93704

5.2 Experiments on NLG tasks

Additionally, we conduct experiments under the natural language generation (NLG) tasks. We fine-tune the Llama3.2-1B model [14], Qwen3-1.7B model [42], and Gemma2-2B model [41] by AdamW [28] with batch size 16 and a cosine learning rate schedule on a 50K subset of the MetaMathQA dataset [53] for 1 epoch. Then, we evaluate the fine-tuned models on the test set of GSM8K [7] and MATH [18]. During fine-tuning, we fix the same random seed in all baselines and set the learning rate to 4×10^{-4} for all LoRA variants, while 5×10^{-5} for FPFT.

For all variants of LoRA, we inject LoRA blocks for all linear sub-modules except lm_head, with rank $r = 8$ and $\alpha = r$ in the main fine-tuning process. For HRP, we set the preheating rank $hrp_rank = 256$ for $hrp_bs = 8$ with $hrp_step = 200$ steps in the same training dataset with the AdamW optimizer under a constant learning rate. Our model is fine-tuned using a standard supervised learning fine-tuning schema for language modeling, where the loss for the input prompt is set to zero. We present more implementation details in Appendix B.

We report the evaluated results in Table 2, which demonstrate the effectiveness of HRP across most large language models. However, we also observe that HRP (and even FPFT) underperforms some other variants in certain specific cases (e.g., Gemma on MATH). This discrepancy is likely attributed to differences between the training and test datasets. To provide further insights, we include loss curves in Appendix C.2, where both HRP achieve significantly lower loss during fine-tuning compared to other LoRA variants (also for FPFT). Additionally, we report the computational cost in Table 3. As shown, HRP incurs negligible additional time compared to the subsequent fine-tuning process, while requiring no extra GPU memory.

6 Conclusion

In this paper, we first theoretically show the important role of LoRA initialization for convergence, where LoRA is likely to achieve random low-rank results with random initialization, and achieve the best low-rank results with a well-formed initialization. Then, to address the problem, we propose HRP, an initialization algorithm that makes LoRA achieve better fine-tuned results. HRP utilizes a few steps of high-rank LoRA optimization for preheating and computes the main singular vectors of the preheated result as initialization for the main LoRA. We further evaluate the effectiveness of HRP through experiments on NLU and NLG tasks and various models, where HRP makes LoRA achieve better performance compared with other initialization strategies.

References

- [1] Josh Achiam, Steven Adler, Sandhini Agarwal, Lama Ahmad, Ilge Akkaya, Florencia Leoni Aleman, Diogo Almeida, Janko Altenschmidt, Sam Altman, Shyamal Anadkat, et al. Gpt-4 technical report. *arXiv preprint arXiv:2303.08774*, 2023.
- [2] Klaudia Bałazy, Mohammadreza Banaei, Karl Aberer, and Jacek Tabor. Lora-xs: Low-rank adaptation with extremely small number of parameters. *arXiv preprint arXiv:2405.17604*, 2024.
- [3] Dan Biderman, Jacob Portes, Jose Javier Gonzalez Ortiz, Mansheej Paul, Philip Greengard, Connor Jennings, Daniel King, Sam Havens, Vitaliy Chiley, Jonathan Frankle, et al. Lora learns less and forgets less. *arXiv preprint arXiv:2405.09673*, 2024.
- [4] Rishi Bommasani, Drew A Hudson, Ehsan Adeli, Russ Altman, Simran Arora, Sydney von Arx, Michael S Bernstein, Jeannette Bohg, Antoine Bosselut, Emma Brunskill, et al. On the opportunities and risks of foundation models. *arXiv preprint arXiv:2108.07258*, 2021.
- [5] Kerim Büyükköyüz. Olora: Orthonormal low-rank adaptation of large language models. *arXiv preprint arXiv:2406.01775*, 2024.
- [6] Yuejie Chi, Yue M Lu, and Yuxin Chen. Nonconvex optimization meets low-rank matrix factorization: An overview. *IEEE Transactions on Signal Processing*, 67(20):5239–5269, 2019.
- [7] Karl Cobbe, Vineet Kosaraju, Mohammad Bavarian, Mark Chen, Heewoo Jun, Lukasz Kaiser, Matthias Plappert, Jerry Tworek, Jacob Hilton, Reiichiro Nakano, Christopher Hesse, and John Schulman. Training verifiers to solve math word problems. *arXiv preprint arXiv:2110.14168*, 2021.
- [8] Yann N Dauphin and Samuel Schoenholz. Metainit: Initializing learning by learning to initialize. *Advances in Neural Information Processing Systems*, 32, 2019.
- [9] Carl Eckart and Gale Young. The approximation of one matrix by another of lower rank. *Psychometrika*, 1(3):211–218, 1936.
- [10] N Filatov and M Kindulov. Low rank adaptation for stable domain adaptation of vision transformers. *Optical Memory and Neural Networks*, 32(Suppl 2):S277–S283, 2023.
- [11] Shi Fu, Yuzhu Chen, Yingjie Wang, and Dacheng Tao. On championing foundation models: From explainability to interpretability. *arXiv preprint arXiv:2410.11444*, 2024.
- [12] Shi Fu, Sen Zhang, Yingjie Wang, Xinmei Tian, and Dacheng Tao. Towards theoretical understandings of self-consuming generative models. *arXiv preprint arXiv:2402.11778*, 2024.
- [13] Xavier Glorot and Yoshua Bengio. Understanding the difficulty of training deep feedforward neural networks. In *Proceedings of the thirteenth international conference on artificial intelligence and statistics*, pages 249–256. JMLR Workshop and Conference Proceedings, 2010.
- [14] Aaron Grattafiori, Abhimanyu Dubey, Abhinav Jauhri, Abhinav Pandey, Abhishek Kadian, Ahmad Al-Dahle, Aiesha Letman, Akhil Mathur, Alan Schelten, Alex Vaughan, et al. The llama 3 herd of models. *arXiv preprint arXiv:2407.21783*, 2024.
- [15] Soufiane Hayou, Nikhil Ghosh, and Bin Yu. The impact of initialization on lora finetuning dynamics. *arXiv preprint arXiv:2406.08447*, 2024.
- [16] Soufiane Hayou, Nikhil Ghosh, and Bin Yu. Lora+: Efficient low rank adaptation of large models. *arXiv preprint arXiv:2402.12354*, 2024.
- [17] Kaiming He, Xiangyu Zhang, Shaoqing Ren, and Jian Sun. Delving deep into rectifiers: Surpassing human-level performance on imagenet classification. In *Proceedings of the IEEE international conference on computer vision*, pages 1026–1034, 2015.
- [18] Dan Hendrycks, Collin Burns, Saurav Kadavath, Akul Arora, Steven Basart, Eric Tang, Dawn Song, and Jacob Steinhardt. Measuring mathematical problem solving with the math dataset. *arXiv preprint arXiv:2103.03874*, 2021.
- [19] Ralph Howard. The gronwall inequality. *lecture notes*, 1998.
- [20] Edward J Hu, Yelong Shen, Phillip Wallis, Zeyuan Allen-Zhu, Yuanzhi Li, Shean Wang, Lu Wang, and Weizhu Chen. Lora: Low-rank adaptation of large language models. *arXiv preprint arXiv:2106.09685*, 2021.

[21] Yuheng Ji, Yue Liu, Zhicheng Zhang, Zhao Zhang, Yuting Zhao, Gang Zhou, Xingwei Zhang, Xinwang Liu, and Xiaolong Zheng. Advlora: Adversarial low-rank adaptation of vision-language models. *arXiv preprint arXiv:2404.13425*, 2024.

[22] Damjan Kalajdzievski. A rank stabilization scaling factor for fine-tuning with lora. *arXiv preprint arXiv:2312.03732*, 2023.

[23] Dawid J Kopiczko, Tijmen Blankevoort, and Yuki M Asano. Vera: Vector-based random matrix adaptation. *arXiv preprint arXiv:2310.11454*, 2023.

[24] Ananya Kumar, Aditi Raghunathan, Robbie Jones, Tengyu Ma, and Percy Liang. Fine-tuning can distort pretrained features and underperform out-of-distribution. *arXiv preprint arXiv:2202.10054*, 2022.

[25] Bingcong Li, Liang Zhang, Aryan Mokhtari, and Niao He. On the crucial role of initialization for matrix factorization. *arXiv preprint arXiv:2410.18965*, 2024.

[26] Haokun Liu, Derek Tam, Mohammed Muqeeth, Jay Mohta, Tenghao Huang, Mohit Bansal, and Colin A Raffel. Few-shot parameter-efficient fine-tuning is better and cheaper than in-context learning. *Advances in Neural Information Processing Systems*, 35:1950–1965, 2022.

[27] Shih-Yang Liu, Chien-Yi Wang, Hongxu Yin, Pavlo Molchanov, Yu-Chiang Frank Wang, Kwang-Ting Cheng, and Min-Hung Chen. Dora: Weight-decomposed low-rank adaptation. *arXiv preprint arXiv:2402.09353*, 2024.

[28] Ilya Loshchilov and Frank Hutter. Decoupled weight decay regularization, 2019.

[29] Grigory Malinovsky, Umberto Michieli, Hasan Abed Al Kader Hammoud, Taha Ceritli, Hayder Elesedy, Mete Ozay, and Peter Richtárik. Randomized asymmetric chain of lora: The first meaningful theoretical framework for low-rank adaptation. *arXiv preprint arXiv:2410.08305*, 2024.

[30] Yuren Mao, Yuhang Ge, Yijiang Fan, Wenyi Xu, Yu Mi, Zhonghao Hu, and Yunjun Gao. A survey on lora of large language models. *Frontiers of Computer Science*, 19(7):197605, 2025.

[31] Fanxu Meng, Zhaohui Wang, and Muhan Zhang. Pissa: Principal singular values and singular vectors adaptation of large language models. *arXiv preprint arXiv:2404.02948*, 2024.

[32] Hancheng Min, Salma Tarmoun, René Vidal, and Enrique Mallada. On the explicit role of initialization on the convergence and implicit bias of overparametrized linear networks. In *International Conference on Machine Learning*, pages 7760–7768. PMLR, 2021.

[33] Dmytro Mishkin and Jiri Matas. All you need is a good init. *arXiv preprint arXiv:1511.06422*, 2015.

[34] Vivak Patel, Shushu Zhang, and Bowen Tian. Global convergence and stability of stochastic gradient descent. *Advances in Neural Information Processing Systems*, 35:36014–36025, 2022.

[35] Kaustubh Ponkshe, Raghav Singhal, Eduard Gorbunov, Alexey Tumanov, Samuel Horvath, and Praneeth Vepakomma. Initialization using update approximation is a silver bullet for extremely efficient low-rank fine-tuning. *arXiv preprint arXiv:2411.19557*, 2024.

[36] Colin Raffel, Noam Shazeer, Adam Roberts, Katherine Lee, Sharan Narang, Michael Matena, Yanqi Zhou, Wei Li, and Peter J. Liu. Exploring the limits of transfer learning with a unified text-to-text transformer. *Journal of Machine Learning Research*, 21(140):1–67, 2020.

[37] Adithya Renduchintala, Tugrul Konuk, and Oleksii Kuchaiev. Tied-lora: Enhacing parameter efficiency of lora with weight tying. *arXiv preprint arXiv:2311.09578*, 2023.

[38] Andrew M Saxe, James L McClelland, and Surya Ganguli. Exact solutions to the nonlinear dynamics of learning in deep linear neural networks. *arXiv preprint arXiv:1312.6120*, 2013.

[39] Yurun Song, Junchen Zhao, Ian G Harris, and Sangeetha Abdu Jyothi. Sharelora: Parameter efficient and robust large language model fine-tuning via shared low-rank adaptation. *arXiv preprint arXiv:2406.10785*, 2024.

[40] Salma Tarmoun, Guilherme Franca, Benjamin D Haeffele, and Rene Vidal. Understanding the dynamics of gradient flow in overparameterized linear models. In *International Conference on Machine Learning*, pages 10153–10161. PMLR, 2021.

[41] Gemma Team. Gemma, 2024.

[42] Qwen Team. Qwen3, April 2025.

[43] Hugo Touvron, Louis Martin, Kevin Stone, Peter Albert, Amjad Almahairi, Yasmine Babaei, Nikolay Bashlykov, Soumya Batra, Prajjwal Bhargava, Shruti Bhosale, et al. Llama 2: Open foundation and fine-tuned chat models. *arXiv preprint arXiv:2307.09288*, 2023.

[44] Sergey Voronin and Per-Gunnar Martinsson. Rsvdpack: An implementation of randomized algorithms for computing the singular value, interpolative, and cur decompositions of matrices on multi-core and gpu architectures. *arXiv preprint arXiv:1502.05366*, 2015.

[45] Alex Wang. Glue: A multi-task benchmark and analysis platform for natural language understanding. *arXiv preprint arXiv:1804.07461*, 2018.

[46] Hongyi Wang, Saurabh Agarwal, and Dimitris Papailiopoulos. Pufferfish: Communication-efficient models at no extra cost. *Proceedings of Machine Learning and Systems*, 3:365–386, 2021.

[47] Hongyi Wang, Saurabh Agarwal, Yoshiki Tanaka, Eric Xing, Dimitris Papailiopoulos, et al. Cuttlefish: Low-rank model training without all the tuning. *Proceedings of Machine Learning and Systems*, 5:578–605, 2023.

[48] Shaowen Wang, Linxi Yu, and Jian Li. Lora-ga: Low-rank adaptation with gradient approximation. *arXiv preprint arXiv:2407.05000*, 2024.

[49] Johan S Wind. Asymmetric matrix sensing by gradient descent with small random initialization. *arXiv preprint arXiv:2309.01796*, 2023.

[50] Wenhan Xia, Chengwei Qin, and Elad Hazan. Chain of lora: Efficient fine-tuning of language models via residual learning. *arXiv preprint arXiv:2401.04151*, 2024.

[51] Yibo Yang, Hong Wang, Haobo Yuan, and Zhouchen Lin. Towards theoretically inspired neural initialization optimization. *Advances in Neural Information Processing Systems*, 35:18983–18995, 2022.

[52] Tian Ye and Simon S Du. Global convergence of gradient descent for asymmetric low-rank matrix factorization. *Advances in Neural Information Processing Systems*, 34:1429–1439, 2021.

[53] Longhui Yu, Weisen Jiang, Han Shi, Jincheng Yu, Zhengying Liu, Yu Zhang, James T Kwok, Zhenguo Li, Adrian Weller, and Weiyang Liu. Metamath: Bootstrap your own mathematical questions for large language models. *arXiv preprint arXiv:2309.12284*, 2023.

[54] Yuchen Zeng and Kangwook Lee. The expressive power of low-rank adaptation. *arXiv preprint arXiv:2310.17513*, 2023.

[55] Qingru Zhang, Minshuo Chen, Alexander Bukharin, Nikos Karampatziakis, Pengcheng He, Yu Cheng, Weizhu Chen, and Tuo Zhao. Adalora: Adaptive budget allocation for parameter-efficient fine-tuning. *arXiv preprint arXiv:2303.10512*, 2023.

[56] Chen Zhu, Renkun Ni, Zheng Xu, Kezhi Kong, W Ronny Huang, and Tom Goldstein. Gradinit: Learning to initialize neural networks for stable and efficient training. *Advances in Neural Information Processing Systems*, 34:16410–16422, 2021.

[57] Jiacheng Zhu, Kristjan Greenewald, Kimia Nadjahi, Haitz Sáez de Ocáriz Borde, Rickard Brüel Gabrielsson, Leshem Choshen, Marzyeh Ghassemi, Mikhail Yurochkin, and Justin Solomon. Asymmetry in low-rank adapters of foundation models. *arXiv preprint arXiv:2402.16842*, 2024.

A Proofs of Theorems

In this section, we present the proof for the theorems above. We begin with some notation, lemmas, and their proofs.

A.1 Notations and Lemmas

For LoRA, what really matters the performance is the multiplied adapters $\frac{\alpha}{r} B_t A_t^\top$, which we denote as X_t . To study the properties of X_t , we define the following auxiliary values:

$$Y_t = \frac{\alpha}{r} A_t A_t^\top, \quad Z_t = \frac{\alpha}{r} B_t B_t^\top, \quad G_t = \frac{\alpha}{r} \nabla_W \mathcal{L}(W + \frac{\alpha}{r} B_t^\top A_t).$$

Then flow 1 can be restated as

$$\begin{cases} dX_t = [-\eta_B G_t Y_t - \eta_A Z_t G_t] dt, \\ dY_t = [-\eta_A G_t^\top X_t - \eta_A X_t^\top G_t] dt, \\ dZ_t = [-\eta_B G_t X_t^\top - \eta_B X_t G_t^\top] dt. \end{cases}$$

With these notations, X_t, Y_t, Z_t has the following properties:

1. Y_t and Z_t are symmetric and semi-positive.
2. $d \text{Trace}(Y_t) = d \text{Trace}(Z_t)$.
3. For zero+random initialization, $X_t = O_{b \times a}$.
4. For zero+random LSI, $Y_t = O_{a \times a}$.
5. For zero+random RSI, $Z_t = O_{b \times b}$.

Besides, we denote $\|\cdot\|_F$ as the Frobenius norm, $U_X \Sigma_X V_X$ as the SVD decomposition of X where $\Sigma_X = \text{diag}(\sigma_1(X), \sigma_2(X), \dots)$ with $\sigma_1(X) \geq \sigma_2(X) \geq \dots$.

Lemma 1. *Gradient flow of matrix factorization 2 with Asymmetric LoRA in LSI ($\eta_A = \eta, \eta_B = 0, A_0 = O_{a \times r}$), X_t has the following closed form:*

$$X_t = [I - e^{-\eta Z_0 t}] M.$$

For matrix factorization 2 with Asymmetric LoRA in RSI ($\eta_A = 0, \eta_B = \eta, B_0 = O_{b \times r}$), X_t has the following closed form:

$$X_t = M [I - e^{-\eta Y_0 t}].$$

Here, e^{matrix} denotes the exponential operation on a matrix.

Proof. For Asymmetric LoRA in LSI, by taking $\eta_A = \eta, \eta_B = 0$ into flow 4, we get

$$\begin{cases} dX_t = [-\eta Z_t G_t] dt, \\ dY_t = [-\eta G_t^\top X_t - \eta X_t^\top G_t] dt, \\ dZ_t = O_{b \times b}. \end{cases}$$

which means $Z_t \equiv Z_0$ for all t , and $\dot{X}_t = -\eta Z_0 (X_t - M)$. Then X_t has an analytic solution

$$X_t = X_0 + [I - e^{-\eta Z_0 t}] M = [I - e^{-\eta Z_0 t}] M.$$

For Asymmetric LoRA in RSI, by taking $\eta_A = 0, \eta_B = \eta$ into flow 4, we get

$$\begin{cases} dX_t = [-\eta G_t Y_t] dt, \\ dY_t = O_{a \times a}, \\ dZ_t = [-\eta G_t X_t^\top - \eta X_t G_t^\top] dt. \end{cases}$$

which means $Y_t \equiv Y_0$ for all t , and $\dot{X}_t = -\eta (X_t - M) Y_0$. Then X_t has an analytic solution

$$X_t = X_0 + M [I - e^{-\eta Y_0 t}] = M [I - e^{-\eta Y_0 t}].$$

□

Lemma 2. *For any matrix $M \in \mathbb{R}^{d_1 \times d_2}$ and any orthogonal matrix $U \in \mathbb{R}^{d_1 \times d_1}$ and $r \leq d_2$, for*

$$X = U \begin{pmatrix} I_r & \\ & O_{(d_1-r) \times (d_1-r)} \end{pmatrix} U^\top M,$$

we have

$$\|M - X\|_F^2 = \|M\|_F^2 - \|X\|_F^2.$$

Proof. We have

$$\|M\|_F^2 = \|X\|_F^2 + \|M - X\|_F^2 + 2 \operatorname{Trace}(X^\top(M - X)).$$

Then it is sufficient to prove $\operatorname{Trace}(X^\top X) = \operatorname{Trace}(X^\top M)$. In fact, we have

$$\begin{aligned} \operatorname{Trace}(X^\top X) &= \operatorname{Trace}\left(M^\top U \begin{pmatrix} I_r & \\ & O_{(d_1-r) \times (d_1-r)} \end{pmatrix} U^\top \cdot U \begin{pmatrix} I_r & \\ & O_{(d_1-r) \times (d_1-r)} \end{pmatrix} U^\top M\right) \\ &= \operatorname{Trace}\left(M^\top U \begin{pmatrix} I_r & \\ & O_{(d_1-r) \times (d_1-r)} \end{pmatrix} U^\top M\right) \\ &= \operatorname{Trace}(X^\top M). \end{aligned}$$

□

Lemma 3. For any matrix $M \in \mathbb{R}^{d_1 \times d_2}$ and any orthogonal matrix $U \in \mathbb{R}^{d_1 \times d_1}$, and all $i, r < \max(d_1, d_2)$, we have

$$\sigma_i \left(U \begin{pmatrix} I_r & \\ & O_{(d_1-r) \times (d_1-r)} \end{pmatrix} U^\top M \right) \leq \sigma_i(M).$$

Proof. For all $v \in \mathbb{R}^{d_2}$, we have

$$\begin{aligned} &\left\| U \begin{pmatrix} I_r & \\ & O_{(d_1-r) \times (d_1-r)} \end{pmatrix} U^\top M v \right\|_F^2 \\ &= \left(U \begin{pmatrix} I_r & \\ & O_{(d_1-r) \times (d_1-r)} \end{pmatrix} U^\top M v \right)^\top \left(U \begin{pmatrix} I_r & \\ & O_{(d_1-r) \times (d_1-r)} \end{pmatrix} U^\top M v \right) \\ &= v^\top M^\top U \begin{pmatrix} I_r & \\ & O_{(d_1-r) \times (d_1-r)} \end{pmatrix} U^\top U \begin{pmatrix} I_r & \\ & O_{(d_1-r) \times (d_1-r)} \end{pmatrix} U^\top M v \\ &= v^\top M^\top U \begin{pmatrix} I_r & \\ & O_{(d_1-r) \times (d_1-r)} \end{pmatrix} U^\top M v \\ &= \sum_{i=1}^r v^\top M^\top u_i u_i^\top M v \\ &= \left(\sum_{i=1}^r v^\top M^\top u_i \right)^2 \\ &\leq \left(\sum_{i=1}^{d_1} v^\top M^\top u_i \right)^2 \\ &= \|Mv\|_F^2. \end{aligned}$$

Then for all space $S \subset \mathbb{R}^{d_2}$, we have

$$\min_{v \in S} \left\| U \begin{pmatrix} I_r & \\ & O_{(d_1-r) \times (d_1-r)} \end{pmatrix} U^\top M v \right\|_F \leq \min_{v \in S} \|Mv\|_F.$$

Thus we have

$$\begin{aligned} \sigma_i \left(U \begin{pmatrix} I_r & \\ & O_{(d_1-r) \times (d_1-r)} \end{pmatrix} U^\top M \right) &= \max_{\substack{S \subset \mathbb{R}^{d_2} \\ \dim(S)=i}} \min_{v \in S} \left\| U \begin{pmatrix} I_r & \\ & O_{(d_1-r) \times (d_1-r)} \end{pmatrix} U^\top M v \right\|_F \\ &\leq \max_{\substack{S \subset \mathbb{R}^{d_2} \\ \dim(S)=i}} \min_{v \in S} \|Mv\|_F \\ &= \sigma_i(M). \end{aligned}$$

□

Lemma 4 (Gronwall's Theorem [19]). *Consider $x_t \geq 0$ and inequality*

$$dx_t \leq [ax_t + f(t)]dt, \quad x_0 = 0.$$

We have

$$x_t \leq e^{at} \int_0^t f(s)e^{-as}ds.$$

Proof. Consider $x_t e^{-at} \geq 0$ and

$$d[x_t e^{-at}] \leq e^{-at}[ax_t + f(t)]dt - ax_t e^{-at}dt = f(t)e^{-at}dt,$$

thus we get

$$\begin{aligned} x_t e^{-at} &\leq x_0 + \int_0^t f(s)e^{-as}ds, \\ x_t &\leq e^{at} \int_0^t f(s)e^{-as}ds. \end{aligned}$$

□

A.2 Proof for Theorem 1

In Theorem 1, the objective is \mathcal{L}_t , which refers to $\frac{1}{2} \left\| \frac{\alpha}{r} B_t A_t^\top - M \right\|^2$. Equivalently, it has the following restatement version.

Theorem 7 (Restatement of theorem 1). *Consider Asymmetric LoRA under objective 2 in gradient flow 1 with the frozen adapter from Gaussian initialization or orthogonal initialization. For LSI and RSI, we have for all $t > 0$:*

$$\mathbb{E}_{LSI} [\|X_t - M\|_F^2] \geq \frac{b-r}{b} \sum_{i=1}^{\min\{a,b\}} \sigma_i(M)^2, \quad \mathbb{E}_{RSI} [\|X_t - M\|_F^2] \geq \frac{a-r}{a} \sum_{i=1}^{\min\{a,b\}} \sigma_i(M)^2,$$

where \mathbb{E} represents the expectation with respect to randomness in initialization. The inequality becomes an equality when $t \rightarrow \infty$.

Proof. For Asymmetric LoRA in LSI with fixed B_0 , according to Lemma 1 we have

$$X_t = [I - e^{-\eta Z_0 t}] M = [I - e^{-\eta B_0 B_0^\top t}] M.$$

For the SVD decomposition $B_0 = U_B \Sigma_B V_B^\top$, we have $Z_0 = U_B (\Sigma_B)^2 U_B^\top$ where Σ_B is a diagonal matrix with only first r elements non-zero. Then, consider $t \rightarrow \infty$, we have

$$\lim_{t \rightarrow \infty} X_t = \lim_{t \rightarrow \infty} [[I - e^{-\eta Z_0 t}] M] \tag{4}$$

$$= [I - \lim_{t \rightarrow \infty} e^{-\eta Z_0 t}] M \tag{5}$$

$$= U_B \left[I - \lim_{t \rightarrow \infty} e^{-\eta \Sigma_B^2 t} \right] U_B^\top M = U_B \begin{pmatrix} I_r & \\ & O_{b-r} \end{pmatrix} U_B^\top M. \tag{6}$$

According to Lemma 2, we have

$$\begin{aligned} \lim_{t \rightarrow \infty} \|X_t - M\|_F^2 &= \left\| \lim_{t \rightarrow \infty} X_t - M \right\|_F^2 = \|M\|_F^2 - \left\| \lim_{t \rightarrow \infty} X_t \right\|_F^2 \\ &= \|M\|_F^2 - \left\| U_B \begin{pmatrix} I_r & \\ & O_{b-r} \end{pmatrix} U_B^\top M \right\|_F^2 \\ &= \|M\|_F^2 - \left\| \begin{pmatrix} I_r & \\ & O_{b-r} \end{pmatrix} U_B^\top M \right\|_F^2 \\ &= \|M\|_F^2 - \sum_{i=1}^r \|u_i(B)^\top M\|_F^2. \end{aligned}$$

For finite t , we have

$$\begin{aligned} \frac{d\|X_t - M\|_F^2}{dt} &= 2 \operatorname{Trace} \left([X_t - M]^\top \frac{d}{dt} [X_t - M] \right) \\ &= 2 \operatorname{Trace} \left([X_t - M]^\top [-\eta Z_0 G_t] \right) \\ &= -2 \frac{\eta \alpha^2}{r^2} \operatorname{Trace} \left([X_t - M]^\top B_0 B_0^\top [X_t - M] \right) \leq 0, \end{aligned}$$

indicating for any fixed B_0 , $\|X_t - M\|_F^2$ is lower bounded by $\lim_{t \rightarrow \infty} \|X_t - M\|_F^2$.

Gaussian initialization and orthogonal initialization share the same probability for the same U_B , thus their properties at converged results are the same. For any orthogonal matrix U , denote $U^{(i)}$ as the matrix that moves the right i column of U to left, i.e. $[U_{[:,i]}, U_{[:,i+1]}, \dots]$ in Python. Due to Gaussian initialization of B , the p.d.f at $U_B = U^{(i)}$ is the same as p.d.f at $U_B = U^{(j)}$ for all i, j . Thus, we have

$$\begin{aligned} \mathbb{E}_{B_0} \lim_{t \rightarrow \infty} \|X_t - M\|_F^2 &= \mathbb{E}_{B_0} \left[\|M\|_F^2 - \sum_{i=1}^r \|u_i(B)^\top M\|_F^2 \right], \\ &= \|M\|_F^2 - \mathbb{E}_U \left. \frac{1}{b} \sum_{j=1}^b \sum_{i=1}^r \|u_i(B)^\top M\|_F^2 \right|_{U_B = U^{(j)}}, \\ &= \|M\|_F^2 - \mathbb{E}_U \left. \frac{1}{b} \sum_{i=1}^r \sum_{j=1}^b \|u_i(U^{(j)})^\top M\|_F^2 \right|, \\ &= \|M\|_F^2 - \frac{1}{b} \sum_{i=1}^r \mathbb{E}_U \|U^\top M\|_F^2, \\ &= \|M\|_F^2 - \frac{r}{b} \|M\|_F^2 = \frac{b-r}{b} \sum_{i=1}^{\min\{a,b\}} \sigma_i(M)^2. \end{aligned}$$

For finite t , we have

$$\mathbb{E}_{B_0} \|X_t - M\|_F^2 \geq \mathbb{E}_{B_0} \lim_{t \rightarrow \infty} \|X_t - M\|_F^2 = \frac{b-r}{b} \sum_{i=1}^{\min\{a,b\}} \sigma_i(M)^2.$$

Asymmetric LoRA in RSI with X_t approximating M , is equivalent with Asymmetric LoRA in LSI with X_t^\top approximating M^\top . Thus for RSI we have

$$\mathbb{E}_{A_0} \|X_t - M\|_F^2 = \mathbb{E}_{B_0} \|X_t^\top - M^\top\|_F^2 \geq \mathbb{E}_{B_0} \lim_{t \rightarrow \infty} \|X_t^\top - M^\top\|_F^2 = \frac{a-r}{a} \sum_{i=1}^{\min\{a,b\}} \sigma_i(M)^2.$$

□

A.3 Proof for Theorem 2

In Theorem 2, the assumption $A_0^\top v_i(M) = O_a$ means $Y_0 v_i(M) = O_a$ while $B_0^\top u_i(M) = O_b$ means $Z_0 u_i(M) = O_b$. In conclusion, $\frac{\alpha}{r} B_t A_t^\top$ can be changed to X_t . Equivalently, it has the following restatement version.

Theorem 8 (Restatement of Theorem 2). *For objective 2 in gradient flow 4, if there exists $i \leq r$ making the initial A_0 and B_0 satisfy $Y_0 v_i(M) = O_a$ and $Z_0 u_i(M) = O_b$, we have for any t :*

$$X_t v_i = O_b, \quad \text{and} \quad X_t^\top u_i = O_a,$$

resulting in for any t :

$$\mathcal{L}_t - \mathcal{L}^* \geq \frac{1}{2} [\sigma_i(M)^2 - \sigma_{r+1}(M)^2] > 0,$$

where $\sigma_i(M)$ is the i -th large singular value of M and $u_i(M), v_i(M)$ are the corresponding left and right singular vector.

Proof. Due to the semi-positive property of Y_0 and Z_0 , we have for $t = 0$:

$$X_t v_i = O_b, \quad Y_t v_i = O_a, \quad X_t^\top u_i = O_a, \quad Z_t^\top u_i = O_b. \quad (7)$$

We then prove 7 true for all $t > 0$. According to induction, it is sufficient to prove each gradient in 7 to be zero for all t that satisfies equations 7. In fact, we have

$$\begin{aligned} \frac{d(X_t v_i)}{dt} &= -\frac{\eta\alpha}{r} Z_t(X_t - M)v_i - \frac{\eta\alpha}{r}(X_t - M)Y_t v_i = \frac{\eta\alpha}{r} Z_t M v_i = \frac{\eta\alpha}{r} \sigma_i(M) Z_t^\top u_i = O_b, \\ \frac{d(Y_t v_i)}{dt} &= -\frac{\eta\alpha}{r} X_t^\top(X_t - M)v_i - \frac{\eta\alpha}{r}(X_t - M)^\top X_t v_i = \frac{\eta\alpha}{r} X_t^\top M v_i = \frac{\eta\alpha}{r} \sigma_i(M) X_t^\top u_i = O_a, \\ \frac{d(X_t^\top u_i)}{dt} &= -\frac{\eta\alpha}{r} [Z_t(X_t - M)]^\top u_i - \frac{\eta\alpha}{r} [(X_t - M)Y_t]^\top u_i = \frac{\eta\alpha}{r} Y_t M^\top u_i = \frac{\eta\alpha}{r} \sigma_i(M) Y_t v_i = O_a, \\ \frac{d(Z_t^\top u_i)}{dt} &= -\frac{\eta\alpha}{r} X_t(X_t - M)^\top u_i - \frac{\eta\alpha}{r}(X_t - M)X_t^\top u_i = \frac{\eta\alpha}{r} X_t M^\top u_i = \frac{\eta\alpha}{r} \sigma_i(M) X_t v_i = O_b. \end{aligned}$$

This means that the composition $\sigma_i(M)u_i(M)v_i(M)^\top$ will not emerge from X_t as t grows up. However, the best low-rank approximation of M requires $\sigma_i(M)u_i v_i^\top$ to be included, which makes the optimization never achieve the best low-rank result. For loss, consider $M' = M - \sigma_i(M)u_i v_i^\top$, we have

$$\begin{aligned} \mathcal{L}_t &= \frac{1}{2} \|X_t - M\|_F^2 \\ &= \frac{1}{2} \text{Trace}((X_t - M' - \sigma_i(M)u_i v_i^\top)(X_t - M' - \sigma_i(M)u_i v_i^\top)^\top) \\ &= \frac{1}{2} \|X_t - M'\|_F^2 + \frac{1}{2} \|\sigma_i(M)u_i v_i^\top\|_F^2 \\ &\geq \frac{1}{2} \sum_{j=r+2}^{\min\{a,b\}} \sigma_j(M)^2 + \frac{1}{2} \sigma_i(M)^2 \\ &= \mathcal{L}^* + \frac{1}{2} [\sigma_i(M)^2 - \sigma_{r+1}(M)^2] \end{aligned}$$

□

A.4 Proof for Theorem 3

In the proof of Theorem 3, we denote all “tilde” variables as those from Asymmetric LoRA, while the without “tilde” as those from classic LoRA. Same problem means a same $W \rightarrow \nabla_W \mathcal{L}$ mapping. By replacing $\frac{\alpha}{r} B_t A_t^\top$ with X_t and its “tilde” version, Theorem 3 has the following restatement version.

Theorem 9 (Restatement of theorem 3). *Consider the gradient flow of classic LoRA X_t and the gradient flow of Asymmetric LoRA \tilde{X}_t in the same zero+random initialization. Assume G_t is bounded by R and is Lipschitz in the Frobenius norm, then the difference between Asymmetric LoRA and classic LoRA is upper bounded by*

$$\|X_t - \tilde{X}_t\|_F = O(\eta^4 R^3 r t^4),$$

for small t when they are under a same gradient calculator.

Proof. For classic LoRA in gradient flow, we have

$$\begin{aligned} \|X_t\|_F^2 &= \left\| \frac{\alpha}{r} B_t A_t^\top \right\|_F^2 \\ &\leq \frac{\alpha^2}{r^2} \|B_t\|_F^2 \|A_t\|_F^2 \\ &= \frac{\alpha^2}{r^2} \text{tr}(B_t B_t^\top) \text{tr}(A_t A_t^\top) \\ &= \text{tr}(Z_t) \text{tr}(Y_t) \\ &\leq r \|Z_t\|_F \|Y_t\|_F \end{aligned}$$

Consider the flow of $x_t = \|Y_t - Y_0\|_F + \|Z_t - Z_0\|_F$, we have

$$\begin{aligned}
\frac{dx_t}{dt} &\leq \left\| \frac{d(Y_t - Y_0)}{dt} \right\|_F + \left\| \frac{d(Z_t - Z_0)}{dt} \right\|_F \\
&\leq 4\eta \|X_t\|_F \|G_t\|_F \\
&\leq 4\eta R \sqrt{r \|Z_t\|_F \|Y_t\|_F} \\
&\leq 4\eta R \sqrt{r} \sqrt{\|Z_t - Z_0\|_F \|Y_t - Y_0\|_F + \|Z_0\|_F \|Y_t - Y_0\|_F + \|Z_t - Z_0\|_F \|Y_0\|_F} \\
&\leq 4\eta R \sqrt{r} \left(x_t + 2\sqrt{\|Z_0\|_F + \|Y_0\|_F} \sqrt{x_t} \right),
\end{aligned}$$

where inequality 8 holds because $\|Z_0\|_F \|Y_0\|_F = 0$ in zero+random initialization strategy. Besides, we have $x_t > 0$ for $t > 0$, which means

$$\frac{d\sqrt{x_t}}{dt} \leq 2\eta R \sqrt{r} \left(\sqrt{x_t} + 2\sqrt{\|Z_0\|_F + \|Y_0\|_F} \right).$$

Through Gronwall Theorem, we have

$$\begin{aligned}
\sqrt{x_t} &\leq e^{2\eta R \sqrt{r} t} \int_0^t 4\eta R \sqrt{r} \sqrt{\|Z_0\|_F + \|Y_0\|_F} e^{-2\eta R \sqrt{r} s} ds \\
&= 2\sqrt{\|Z_0\|_F + \|Y_0\|_F} e^{2\eta R \sqrt{r} t} \left(1 - e^{-2\eta R \sqrt{r} t} \right) \\
\|Y_t - Y_0\|_F + \|Z_t - Z_0\|_F &\leq 2(\|Z_0\|_F + \|Y_0\|_F) \left(e^{2\eta R \sqrt{r} t} - 1 \right)^2.
\end{aligned}$$

Considering the difference to gradient flow of Asymmetric LoRA \tilde{X}_t , we have

$$\begin{aligned}
\frac{d \left\| X_t - \tilde{X}_t \right\|_F}{dt} &\leq \left\| \frac{d[X_t - \tilde{X}_t]}{dt} \right\|_F \\
&\leq \left\| -\eta(Z_t - Z_0)G_t - \eta Z_0(G_t - \tilde{G}_t) - \eta G_t(Y_t - Y_0) - \eta(G_t - \tilde{G}_t)Y_0 \right\|_F \\
&\leq \eta \left[\|G_t\|_F (\|Y_t - Y_0\|_F + \|Z_t - Z_0\|_F) + (\|Z_0\|_F + \|Y_0\|_F) \|G_t - \tilde{G}_t\|_F \right] \\
&\leq \eta \left[2R(\|Z_0\|_F + \|Y_0\|_F) \left(e^{2\eta R \sqrt{r} t} - 1 \right)^2 + L(\|Z_0\|_F + \|Y_0\|_F) \|X_t - \tilde{X}_t\|_F \right].
\end{aligned}$$

Through Gronwall Theorem, we have

$$\begin{aligned}
\left\| X_t - \tilde{X}_t \right\|_F &\leq \int_0^t 2\eta R e^{\eta L(\|Z_0\|_F + \|Y_0\|_F)(t-s)} (\|Z_0\|_F + \|Y_0\|_F) \left(e^{2\eta R \sqrt{r} s} - 1 \right)^2 ds \\
&\leq 2\eta R t e^{\eta L(\|Z_0\|_F + \|Y_0\|_F)t} (\|Z_0\|_F + \|Y_0\|_F) \left(e^{2\eta R \sqrt{r} t} - 1 \right)^2 \\
&= O(\eta^4 R^3 t^4)
\end{aligned}$$

□

A.5 Proof for Theorem 4

In the Theorem 4, by replacing A_0 initialization to Y_0 initialization and B_0 initialization to Z_0 initialization, it has the following restatement version.

Theorem 10 (Restatement of theorem 4). *Consider Asymmetric LoRA under objective 2 in gradient flow 4. For RSI with $Y_0 = \frac{\alpha}{r} V_M \text{diag}(I_r, O_{(a-r) \times (a-r)}) V_M^\top$, $Z_0 = O_{b \times b}$ or LSI with $Y_0 = O_{a \times a}$, $Z_0 = \frac{\alpha}{r} U_M \text{diag}(I_r, O_{(b-r) \times (b-r)}) U_M^\top$, we have*

$$\mathcal{L}_t - \mathcal{L}^* = O \left(\exp \left\{ -\frac{2\alpha\eta}{r} t \right\} \right).$$

Proof. According to Lemma 1, with LSI initialization, we have

$$X_t = M[I - e^{-\eta Z_0 t}] = (1 - e^{-\frac{\alpha\eta}{r}t})MV_M \begin{pmatrix} I_r & \\ & O_{(a-r) \times (a-r)} \end{pmatrix} V_M^\top,$$

which has loss

$$\begin{aligned} \mathcal{L}(X_t) &= \frac{1}{2} \|X_t - M\|_F^2 \\ &= \frac{1}{2} \left\| M - (1 - e^{-\frac{\alpha\eta}{r}t})MV_M \begin{pmatrix} I_r & \\ & O_{(a-r) \times (a-r)} \end{pmatrix} V_M^\top \right\|_F^2 \\ &= \frac{1}{2} \left\| U_M \Sigma_M V_M^\top - (1 - e^{-\frac{\alpha\eta}{r}t})U_M \Sigma_M \begin{pmatrix} I_r & \\ & O_{(a-r) \times (a-r)} \end{pmatrix} V_M^\top \right\|_F^2 \\ &= \frac{1}{2} \left\| \Sigma_M - (1 - e^{-\frac{\alpha\eta}{r}t})\Sigma_M \begin{pmatrix} I_r & \\ & O_{(a-r) \times (a-r)} \end{pmatrix} \right\|_F^2 \\ &= \frac{1}{2} \left\| \Sigma_M \begin{pmatrix} e^{-\frac{\alpha\eta}{r}t} I_r & \\ & I_{a-r} \end{pmatrix} \right\|_F^2 \\ &= \frac{1}{2} e^{-\frac{2\alpha\eta}{r}t} \sum_{i=1}^r \sigma_i(M)^2 + \frac{1}{2} \sum_{i=r+1}^{\min\{a,b\}} \sigma_i(M)^2 \\ &= O\left(\exp\left\{-\frac{2\alpha\eta}{r}t\right\}\right) + \mathcal{L}^*. \end{aligned}$$

Asymmetric LoRA in RSI with X_t approximating M , is equivalent with Asymmetric LoRA in LSI with X_t^\top approximating M^\top . Thus for RSI we also have

$$\mathcal{L}_t - \mathcal{L}^* = O\left(\exp\left\{-\frac{2\alpha\eta}{r}t\right\}\right).$$

□

A.6 Proof for Theorem 5

In the Theorem 5, by replacing A_0 initialization to Y_0 initialization and B_0 initialization to Z_0 initialization, it has the following restatement version.

Theorem 11 (Restatement of theorem 5). *Consider classic LoRA under objective 2 in gradient flow 4. For initialization same as Theorem 10, we have*

$$\mathcal{L}_t - \mathcal{L}^* = O\left(\exp\left[\frac{-\alpha\eta t}{r} \left(1 + \sqrt{1 + \frac{2r^2}{\alpha^2} \sigma_r(M)^2 \left[1 - e^{-\frac{\alpha\eta t}{2r}}\right]^2}\right)\right]\right).$$

where $\sigma_i(M)$ is the i -th singular value of M and is defined in Theorem 2.

Proof. We consider

$$\hat{X}_t := U_M^\top X_t V_M, \quad \hat{Y}_t := V_M^\top Y_t V_M, \quad \hat{Z}_t := U_M^\top Z_t U_M, \quad (8)$$

and first prove

$$\forall r, \hat{X}_t, \hat{Y}_t, \hat{Z}_t \text{ are diagonal matrices with only the first } r \text{ elements non-zero.} \quad (9)$$

If initialized with RSI, i.e. $Y_0 = \frac{\alpha}{r} V_M \text{ diag}\left(I_r, O_{(a-r) \times (a-r)}\right) V_M^\top, Z_0 = O_{b \times b}$, then we have

$$\hat{X}_t := U_M^\top X_0 V_M = O_{b \times a}, \quad \hat{Y}_t := V_M^\top Y_0 V_M = \frac{\alpha}{r} \begin{pmatrix} I_r & \\ & O_{a-r} \end{pmatrix}, \quad \hat{Z}_t := U_M^\top Z_0 U_M = O_{b \times b}.$$

If initialized with LSI, i.e. $Y_0 = O_{a \times a}, Z_0 = \frac{\alpha}{r} U_M \text{ diag}\left(I_r, O_{(b-r) \times (b-r)}\right) U_M^\top$, then we have

$$\hat{X}_t := U_M^\top X_0 V_M = O_{b \times a}, \quad \hat{Y}_t := V_M^\top Y_0 V_M = O_{a \times a}, \quad \hat{Z}_t := U_M^\top Z_0 U_M = \frac{\alpha}{r} \begin{pmatrix} I_r & \\ & O_{b-r} \end{pmatrix}.$$

Thus, claim 9 is true for $t = 0$. If it is true for t , then their gradient satisfies

$$\begin{aligned}\dot{\hat{X}}_t &= U_M^\top [-\eta Z_t(X_t - M) - \eta(X_t - M)Y_t] V_M = -\eta \hat{Z}_t(\hat{X}_t - \Sigma_M) - \eta(\hat{X}_t - \Sigma_M)\hat{Y}_t, \\ \dot{\hat{Y}}_t &= V_M^\top [-\eta X_t^\top(X_t - M) - \eta(X_t - M)^\top X_t] V_M = -\eta \hat{X}_t^\top(\hat{X}_t - \Sigma_M) - \eta(\hat{X}_t - \Sigma_M)^\top \hat{X}_t, \\ \dot{\hat{Z}}_t &= U_M^\top [-\eta X_t(X_t - M)^\top - \eta(X_t - M)X_t^\top] U_M = -\eta \hat{X}_t(\hat{X}_t - \Sigma_M)^\top - \eta(\hat{X}_t - \Sigma_M)\hat{X}_t^\top,\end{aligned}$$

which are all diagonal matrices with only the first r elements non-zero. Thus, claim 9 is true for all t . We denote the i -th diagonal elements for $\hat{X}_t, \hat{Y}_t, \hat{Z}_t$ as $x_{t,i}, y_{t,i}, z_{t,i}$. Then for each i , we have

$$\begin{aligned}\dot{x}_{t,i} &= -\eta z_{t,i}(x_{t,i} - \sigma_i(M)) - \eta(x_{t,i} - \sigma_i(M))y_{t,i} = -\eta(y_{t,i} + z_{t,i})(x_{t,i} - \sigma_i(M)), \\ \dot{y}_{t,i} &= \dot{z}_{t,i} = -\eta x_{t,i}(x_{t,i} - \sigma_i(M)) - \eta(x_{t,i} - \sigma_i(M))x_{t,i} = -2\eta x_{t,i}(x_{t,i} - \sigma_i(M)),\end{aligned}$$

and they are independent with other $j \neq i$. Consider

$$\begin{aligned}d[(y_{t,i} + z_{t,i})^2] &= -4\eta(y_{t,i} + z_{t,i})x_{t,i}(x_{t,i} - \sigma_i(M)) \\ &= -4\eta x_{t,i}(y_{t,i} + z_{t,i})(x_{t,i} - \sigma_i(M)) = 2d[x_{t,i}^2],\end{aligned}$$

resulting in

$$y_{t,i} + z_{t,i} = \sqrt{(y_{0,i} + z_{0,i})^2 + 2x_{t,i}^2 - 2x_{0,i}^2} = \sqrt{\frac{\alpha^2}{r^2} + 2x_{t,i}^2}.$$

So, the dynamic of $x_{t,i}$ is

$$\dot{x}_{t,i} = -\eta(y_{t,i} + z_{t,i})(x_{t,i} - \sigma_i(M)) = -\eta(x_{t,i} - \sigma_i(M))\sqrt{\frac{\alpha^2}{r^2} + 2x_{t,i}^2}.$$

For a fixed i , consider another flow x_t with some s , which satisfies

$$\begin{aligned}x_0 &= x_{0,i} \\ \dot{x}_t &= -\eta(x_t - \sigma_i(M))\frac{\alpha}{r}, \quad 0 < t < s, \\ \dot{x}_t &= -\eta(x_t - \sigma_i(M))\sqrt{\frac{\alpha^2}{r^2} + 2x_s^2}, \quad s < t.\end{aligned}$$

Then we have always $x_{t,i} \geq x_i$ and $(\sigma_i(M) - x_{t,i})^2 \leq (\sigma_i(M) - x_t)^2$. We can get $x_s = \sigma_i(M)[1 - e^{-\frac{\alpha\eta s}{r}}]$, and for $t > s$:

$$x_t = \sigma_i(M) \left[1 - \exp \left[\frac{-\alpha\eta s}{r} - \eta(t-s)\sqrt{\frac{\alpha^2}{r^2} + 2x_s^2} \right] \right].$$

By setting $t = 2s$, we have

$$\begin{aligned}x_{2s,i} &\geq x_{2s} = \sigma_i(M) \left[1 - \exp \left[\frac{-\alpha\eta s}{r} \left(1 + \sqrt{1 + \frac{2r^2}{\alpha^2}x_s^2} \right) \right] \right] \\ &= \sigma_i(M) \left[1 - \exp \left[\frac{-\alpha\eta s}{r} \left(1 + \sqrt{1 + \frac{2r^2}{\alpha^2}\sigma_i(M)^2[1 - e^{-\frac{\alpha\eta s}{r}}]^2} \right) \right] \right] \\ &\geq \sigma_i(M) \left[1 - \exp \left[\frac{-\alpha\eta s}{r} \left(1 + \sqrt{1 + \frac{2r^2}{\alpha^2}\sigma_r(M)^2[1 - e^{-\frac{\alpha\eta s}{r}}]^2} \right) \right] \right].\end{aligned}$$

So, for X_t , we have

$$\begin{aligned}
\mathcal{L}_t - \mathcal{L}^* &= \frac{1}{2} \|U_M \hat{X}_t V_M^\top - M\|_F^2 - \mathcal{L}^* \\
&= \|\hat{X}_t - \Sigma_M\|_F^2 - \mathcal{L}^* \\
&= \sum_{i=1}^r (\sigma_i(M) - x_{t,i})^2 \\
&\leq \sum_{i=1}^r \sigma_i(M)^2 \exp \left[\frac{-\alpha\eta t}{2r} \left(1 + \sqrt{1 + \frac{2r^2}{\alpha^2} \sigma_r(M)^2 \left[1 - e^{-\frac{\alpha\eta t}{2r}} \right]^2} \right) \right]^2 \\
&= O \left(\exp \left[\frac{-\alpha\eta t}{r} \left(1 + \sqrt{1 + \frac{2r^2}{\alpha^2} \sigma_r(M)^2 \left[1 - e^{-\frac{\alpha\eta t}{2r}} \right]^2} \right) \right] \right)
\end{aligned}$$

□

A.7 Proof for Theorem 6

We prove Theorem 6 in the notation of X_t, Y_t, Z_t . First, we restate this theorem and HRP algorithm.

Theorem 12 (Restatement of theorem 6). *For one LSI Asymmetric LoRA \hat{X}_t with rank $\text{hrp_rank} \geq r$ and random orthogonal initialization*

$$\hat{A}_0 = O_{a \times r}, \hat{B}_0 = \sum_{i=1}^{\text{hrp_rank}} \hat{u}_i e_{i, \text{hrp_rank}},$$

And another RSI Asymmetric LoRA X_s with initialization

$$\hat{A}_0 = \sum_{i=1}^{\text{hrp_rank}} v_i (\hat{X}_t) e_{i, \text{hrp_rank}}^\top, \hat{B}_0 = O_{b \times r}.$$

We have for all t , X_s converges to X_∞ with loss in expectation

$$\mathbb{E}_U \mathcal{L}_\infty \leq \sum_{i=r+1}^{\text{hrp_rank}} \sigma_i(M)^2 + \frac{a - \text{hrp_rank}}{2a} \sum_{i=1}^{\max(a, b)} \sigma_i(M)^2.$$

Proof. According to Lemma 1, for the preheating orth-init LSI we have

$$\begin{aligned}
\hat{X}_t &= \left[I - e^{-\eta \hat{Z}_0 t} \right] M \\
&= (1 - e^{-\frac{\alpha\eta t}{r}}) U_{\hat{Z}_0} \begin{pmatrix} I_{\text{hrp_rank}} & \\ & O_{(b-\text{hrp_rank}) \times (b-\text{hrp_rank})} \end{pmatrix} U_{\hat{Z}_0}^\top M \\
&= (1 - e^{-\frac{\alpha\eta t}{r}}) \hat{X}_\infty.
\end{aligned}$$

For the following HRP derived RSI, we have

$$\begin{aligned}
X_t &= M \left[I - e^{-\eta \hat{Y}_0 t} \right] \\
&= (1 - e^{-\frac{\alpha\eta t}{r}}) M V_{\hat{X}_t} \begin{pmatrix} I_r & \\ & O_{(a-r) \times (a-r)} \end{pmatrix} V_{\hat{X}_t}^\top \\
&= (1 - e^{-\frac{\alpha\eta t}{r}}) M V_{X_\infty} \begin{pmatrix} I_r & \\ & O_{(a-r) \times (a-r)} \end{pmatrix} V_{X_\infty}^\top \\
&= \left(1 - e^{-\frac{\alpha\eta t}{r}} \right) X_\infty.
\end{aligned}$$

According to Lemma 2, we have

$$\begin{aligned}
\|X_t\|_F^2 &\geq \left\| U_{\hat{Z}_0} \begin{pmatrix} I_{\text{hrp_rank}} & \\ & O_{(b-\text{hrp_rank}) \times (b-\text{hrp_rank})} \end{pmatrix} U_{\hat{Z}_0}^\top X_t \right\|_F^2 \\
&= \left(1 - e^{-\frac{\alpha \eta t}{r}}\right)^2 \left\| \hat{X}_\infty V_{\hat{X}_\infty} \begin{pmatrix} I_r & \\ & O_{(a-r) \times (a-r)} \end{pmatrix} V_{\hat{X}_\infty}^\top \right\|_F^2 \\
&= \left(1 - e^{-\frac{\alpha \eta t}{r}}\right)^2 \left(\|\hat{X}_\infty\|_F^2 - \sum_{i=r+1}^{\text{hrp_rank}} \sigma_i(\hat{X}_\infty)^2 \right).
\end{aligned}$$

Thus $\|X_\infty - M\|_F^2$ is upper bounded by

$$\|X_\infty - M\|_F^2 \leq \|M\|_F^2 - \|X_\infty\|_F^2 \leq \|M\|_F^2 - \|\hat{X}_\infty\|_F^2 + \sum_{i=r+1}^{\text{hrp_rank}} \sigma_i(\hat{X}_\infty)^2.$$

According to Lemma 3, we have

$$\sigma_i(\hat{X}_\infty) \leq \sigma_i(M),$$

indicating

$$\begin{aligned}
\|X_\infty - M\|_F^2 &\leq \|M\|_F^2 - \|\hat{X}_\infty\|_F^2 + \sum_{i=r+1}^{\text{hrp_rank}} \sigma_i(\hat{X}_\infty)^2 \\
&\leq \|M - \hat{X}_\infty\|_F^2 + \sum_{i=r+1}^{\text{hrp_rank}} \sigma_i(M)^2.
\end{aligned}$$

By taking expectation to both side, according to Theorem 1, we have

$$\mathbb{E}_U \mathcal{L}_\infty \leq \sum_{i=r+1}^{\text{hrp_rank}} \sigma_i(M)^2 + \frac{a - \text{hrp_rank}}{2a} \sum_{i=1}^{\max(a,b)} \sigma_i(M)^2.$$

□

B More Experiment Details

For the GLUE benchmark using the T5-base model, we use the AdamW optimizer with a linear learning rate scheduler with batch size 32 for all tasks and fine-tuning strategies. For LoRA variants, we inject LoRA to all query and value blocks with $r = 4$ and $\alpha = 4$. For FPFT, we use a relatively lower learning rate 5×10^{-5} for all tasks, while for AdaLoRA, we use a relatively higher learning rate 5×10^{-3} . For other LoRA variants, we set the learning rate to the same in each task. Due to the difference across tasks, we set different training epochs and the LoRA learning rate same for all tasks. The detailed information is shown in Table 4.

Table 4: Hyperparameter settings for fine-tuning T5-base on GLUE.

	CoLA	MRPC	QNLI	RTE	STS-B
Learning rate	2×10^{-3}	2×10^{-4}	5×10^{-4}	2×10^{-3}	2×10^{-3}
Epochs	10	20	5	20	10

For the math reasoning tasks using a large language model, we use AdamW optimizer with a cosine learning rate scheduler with batch size 16 for all models and fine-tuning strategies. For LoRA variants, we inject LoRA to all linear blocks except the language model head with $r = 8$ and $\alpha = 8$. For FPFT, we use a relatively lower learning rate 5×10^{-5} for all models, while for LoRA variants, we use a relatively higher learning rate 4×10^{-4} . During fine-tuning, the base model is loaded with the bfloat16 data type, while LoRA blocks are loaded in the float32 data type. In the inference stage, we set the temperature to 0.8, top-p to 0.95, and let the model output no more than 512 tokens.

Table 5: Ablation studies for hrp_rank with hrp_step keeping 100.

hrp_rank	CoLA	MRPC	QNLI	RTE	STS-B	Avg.
8	54.77 \pm 0.04	88.81 \pm 1.14	92.13 \pm 0.10	73.32 \pm 2.66	88.35 \pm 0.52	79.68 \pm 0.53
16	55.08 \pm 1.68	88.73 \pm 0.53	91.97 \pm 0.19	74.73 \pm 0.88	88.68 \pm 0.65	79.84 \pm 0.43
32	55.36 \pm 1.82	88.56 \pm 0.31	92.07 \pm 0.36	74.57 \pm 1.45	88.84 \pm 0.76	79.88 \pm 0.43
64	56.17 \pm 0.43	88.48 \pm 0.35	92.09 \pm 0.14	74.25 \pm 1.45	88.87 \pm 0.43	79.97 \pm 0.25
128	56.18 \pm 0.09	88.89 \pm 0.61	92.23 \pm 0.08	74.25 \pm 1.90	89.04 \pm 0.16	80.12 \pm 0.52

Table 6: Ablation studies for hrp_step with hrp_rank keeping 128.

hrp_step	CoLA	MRPC	QNLI	RTE	STS-B	Avg.
0	54.84 \pm 0.27	88.48 \pm 0.53	91.95 \pm 0.16	73.89 \pm 2.74	88.87 \pm 0.11	79.60 \pm 0.57
50	56.32 \pm 1.28	88.81 \pm 0.61	92.10 \pm 0.28	75.09 \pm 2.34	88.92 \pm 0.24	80.25 \pm 0.63
100	56.18 \pm 0.09	88.89 \pm 0.61	92.23 \pm 0.08	74.25 \pm 1.90	89.04 \pm 0.16	80.12 \pm 0.52
150	56.17 \pm 1.38	88.64 \pm 0.81	92.20 \pm 0.11	76.41 \pm 1.51	88.98 \pm 0.63	80.48 \pm 0.51
200	57.12 \pm 0.65	87.83 \pm 0.76	92.24 \pm 0.19	74.25 \pm 0.95	89.22 \pm 0.69	80.13 \pm 0.42

C Additional Experimental Results

C.1 Ablation Studies

We conducted ablation studies to evaluate how HRP hyperparameters impact the fine-tuned results. First, we fix $hrp_step = 100$ and examined the effect of hrp_rank . As shown in Table 5, HRP performance is not much sensitive to hrp_rank . In CoLA, STS-B, the average score, and QNLI for $hrp_rank \geq 16$, a higher hrp_rank correlates with better performance, indicating a higher hrp_rank is required for better initialization. However, in smaller datasets like RTE and MRPC, this trend is not observed, likely because a lower hrp_rank is enough for these tasks.

We also conducted experiments by fixing $hrp_rank = 128$ to analyze the impact of hrp_step . As shown in Table 6, where $hrp_step = 0$ corresponds to random orthogonal initialization, HRP performance is also not sensitive to hrp_step when HRP is active. However, whether HRP is active or not has a significant impact. This is as expected, as a higher hrp_step is used to mitigate the influence of gradient noise.

C.2 Loss Curves

To provide deeper insights into the training dynamics, we present the loss curve for Llama in Figure 2, Qwen in Figure 3, and Gemma in Figure 4. The visualization convincingly validates our theoretical analysis, demonstrating that HRP indeed achieves superior converged results initialization. Besides, the loss curves reveal that HRP also accelerates the convergence of LoRA, especially in the beginning stage of fine-tuning.

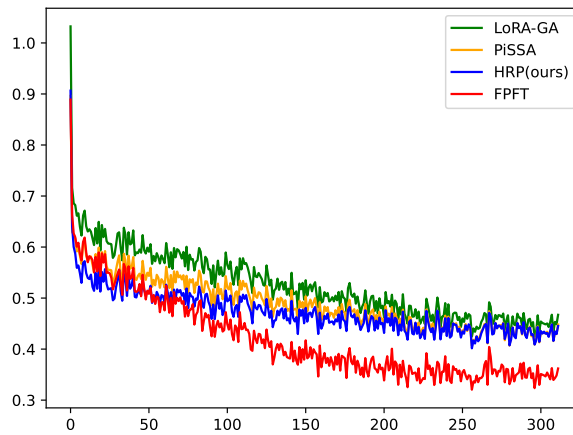


Figure 2: Loss curves for fine-tuning meta-llama/Llama-3.2-1B-Instruct on the MetaMathQA.

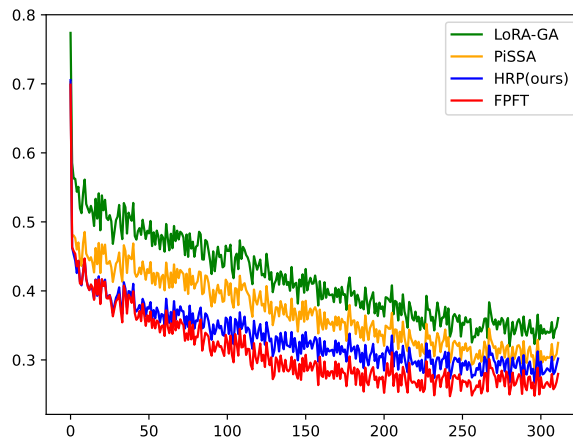


Figure 3: Loss curves for fine-tuning Qwen/Qwen3-1.7B on the MetaMathQA.

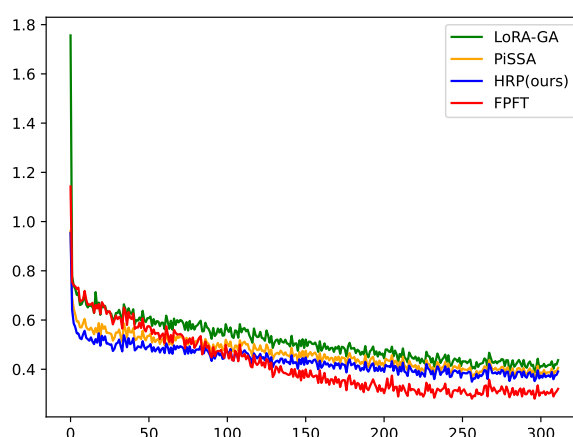


Figure 4: Loss curves for fine-tuning google/gemma-2-2b-it on the MetaMathQA.